

Oxidation Selectivity between *n*-Hexane and Sulfur Dioxide in Diesel Simulated Exhaust Gas over Platinum-Supported Zirconia Catalyst

Yasutaka Nagai, Hirofumi Shinjoh, Koji Yokota

ディーゼル排気モデルガス中でのPt/ZrO₂触媒による*n*-ヘキサンと二酸化硫黄の酸化反応選択性

長井康貴, 新庄博文, 横田幸治

Abstract

A highly selective oxidation performance, which has a higher oxidation activity for hydrocarbons than that for SO₂, is required for diesel oxidation catalysts. We examined the oxidation reaction of *n*-C₆H₁₄ and SO₂ over two types of Pt/ZrO₂ catalysts with low (8 m²/g) and high (75 m²/g) surface areas of the ZrO₂ supports (referred to as ZrO₂-8 and ZrO₂-75, respectively). The Pt/ZrO₂-75 exhibited a desirably higher selectivity for the complete oxidation of *n*-C₆H₁₄ than that of SO₂, as compared with the Pt/ZrO₂-8. In order to clarify the cause of this selective oxidation, we investigated the Arrhenius

parameter for these oxidation reactions and characterized these catalysts using XPS, XRD, TEM, IR and CO₂-TPD methods. The amount of Pt⁰ (metal) in the Pt/ZrO₂-75 was significantly lower than that in Pt/ZrO₂-8, because the high basicity of the ZrO₂-75 support stabilized the high oxidation state of Pt such as Pt²⁺ and Pt⁴⁺. It was concluded that the difference in the number of Pt⁰ sites as catalytic active sites causes the apparent selectivity to change due to the much slower reaction rate for the SO₂ oxidation than that for the *n*-C₆H₁₄ oxidation.

Keywords

Diesel engine, Sulfur dioxide oxidation, Hydrocarbon oxidation, Oxidation selectivity, Platinum/zirconia

要 旨

ディーゼルエンジン用の酸化浄化触媒には、排ガス中の炭化水素は酸化し、SO₂は酸化しない選択的酸化能が要求される。本研究では、ZrO₂担体の比表面積が異なる(8 m²/gおよび75 m²/g、これらをZrO₂-8およびZrO₂-75と記す)2種のPt/ZrO₂触媒による*n*-C₆H₁₄およびSO₂の酸化反応を調べた。Pt/ZrO₂-75触媒はSO₂より*n*-C₆H₁₄を選択的に酸化し、Pt/ZrO₂-8触媒に比べて望ましい選択性を示した。この選択性の原因を明らかにするために、これら酸化反応のアレニウスパラメータを求め、ま

た、XPS、XRD、TEM、IRおよびCO₂-TPD解析により触媒のキャラクタリゼーションを行った。ZrO₂-75の高い塩基性によってPtがPt²⁺およびPt⁴⁺の高酸化状態に保たれるため、Pt/ZrO₂-75中のPt⁰(メタル)サイトの数がPt/ZrO₂-8に比べて著しく減少することがわかった。SO₂酸化反応の速度が*n*-C₆H₁₄に比べて非常に遅いために、触媒活性点として働くPt⁰サイト数の差によって、見かけ上の選択性が変化すると結論された。

キーワード

ディーゼルエンジン, SO₂酸化, 炭化水素酸化, 酸化反応選択性, 白金/ジルコニア

1. Introduction

Diesel emissions are composed of three phases; (1) solids (carbon or soot); (2) liquids (soluble organic fraction and liquid sulfate); and (3) gases (CO, hydrocarbon compounds, NO_x and SO₂). The complete oxidation of carbon, CO and hydrocarbon (HC) compounds is required for the diesel oxidation catalyst^{1, 2)}. However, any sulfur compound contained in the diesel fuel is oxidized to SO₂ during the engine combustion cycle. In the presence of an oxidation catalyst, SO₂ is further oxidized to SO₃, which quickly reacts with the moisture in the exhaust to form sulfate. The sulfate leads to an increase in the weight of the total particulates emitted from the diesel engine and also causes acid rain. Therefore, a highly selective oxidation catalyst, which has a higher oxidation activity for carbon, CO and HC compounds than that for SO₂, is required.

Although it is important to investigate the key factor in developing a highly selective oxidation catalyst, surprisingly, few studies have been conducted³⁾. In this study, we examined the oxidation of *n*-hexane (gaseous HC) and SO₂ over two types of Pt/ZrO₂ catalysts with low and high ZrO₂ support surface areas. These Pt/ZrO₂ catalysts exhibited different selectivities for the oxidation of *n*-hexane and SO₂⁴⁾. The purpose of this study is to clarify the cause of this oxidation selectivity. For this purpose, we investigated the Arrhenius parameter for this oxidation reaction and characterized the catalysts using XPS, XRD, TEM, IR and CO₂-TPD methods⁵⁾.

We employed *n*-hexane as a gaseous HC, because many *n*-alkane species are contained in the exhaust gas phase⁶⁾. A number of studies have been conducted on the complete catalytic oxidation of the C₁-C₃ hydrocarbons such as methane, ethane, propane, etc.^{e.g., 7-11)}. Actual exhaust gases include alkanes with a carbon number higher than C₃. Therefore, we chose *n*-hexane as the HC species. Besides, few studies on the complete catalytic oxidation of hexane (C₆) have been reported. In addition to the foregoing main purpose of clarifying the cause of the reaction selectivity, another purpose of this study is to estimate the complete oxidation of *n*-

hexane over platinum catalysts.

2. Experimental

2.1 Catalyst preparation

The two types of Pt/ZrO₂ catalysts examined for this study are summarized in **Table 1** with the corresponding BET surface areas and ZrO₂ phase. The low surface area zirconia (referred as to ZrO₂-8) was supplied by Mitsuwa Chemicals, Japan. On the other hand, the high surface area zirconia (referred as to ZrO₂-75) was prepared by calcining Zr(OH)₄ (Hayashi Pure Chemical Industries, Japan) in air at 500°C for 3 h. The Pt/ZrO₂ catalysts were prepared by the wet impregnation of ZrO₂ powders with a Pt(NH₃)₂(NO₂)₂ (Tanaka Precious Metals, Japan) aqueous solution. The impregnated powders were dried overnight at 110°C and calcined at 500°C for 3 h in air. The amount of Pt loading of these catalysts was 0.64 wt.%. Also, Pt/SiO₂ (SiO₂ Nippon Aerosil Co., Ltd., specific surface area: 50 m²/g) catalysts with several Pt loading amounts were prepared as references. The catalysts for the activity measurements were pressed into disks and pulverized to 1.0-2.0 mm size.

2.2 Activity measurement

The catalytic activity was determined by using a conventional fixed-bed flow reactor at atmospheric pressure. The reaction temperature was detected by a thermocouple inserted into the catalyst bed, and controlled from 500°C to 150°C at a rate of -6°C min⁻¹. The simulated exhaust gas was composed of 100 ppm *n*-hexane, 50 ppm SO₂, 10 % O₂, 5 % CO₂,

Table 1 The Pt/ZrO₂ catalysts, the BET surface areas and phase identification of ZrO₂.

Catalyst ^a	Pt loading (wt. %)	BET surface area of ZrO ₂ (m ² / g)	Phase of ZrO ₂
Pt/ZrO ₂ -8	0.64	8	Monoclinic
Pt/ZrO ₂ -75	0.64	75	Tetragonal + Monoclinic

^a For catalyst description, see Experimental.

10 % H₂O and the balance N₂. The total flow rate was 8.36 l/min and 3.6 g of catalyst was used. The concentration of the HC and SO₂ were continuously analyzed by a flame ionization detector and a flame photometric detector, respectively. The pre-treatment was carried out at 500°C in the same flowing gas until the conversions of HC and SO₂ became constant. The conversions of HC and SO₂ were calculated based on the following equation:

$$\text{Conversion(\%)} = (X_{\text{in}} - X_{\text{out}}) / X_{\text{in}} \times 100 \dots \dots (1)$$

where X_{in} and X_{out} are the concentrations of HC or SO₂ entering and leaving the catalyst bed, respectively.

The Arrhenius parameter measurements were made using the same above-mentioned conditions, except using the feed gas without CO₂ and H₂O. The Arrhenius parameters were calculated from the conversions of HC and SO₂ at less than about 15%.

2. 3 Catalyst characterization

2. 3. 1 Surface area measurements

The specific surface areas of the samples were estimated using the N₂ adsorption isotherm at 77 K by the one-point Brunauer-Emmett-Teller (BET) method with an automatic surface analyzer (Micro Sorp 4232II from Micro Data Co., Ltd.). The samples were degassed in flowing N₂ at 200°C for 20 min.

2. 3. 2 X-Ray diffraction (XRD)

The powder XRD experiments were carried out using a RINT2000 (Rigaku Co., Ltd.) diffractometer with Cu-K_α radiation (1.5406 Å). The catalyst powder samples were pressed into wafers and affixed to standard-sized microscope slides. The identification of the phase was made by comparison to the JCPDS cards (Joint Committee on Powder Diffraction Standards). The average particle size of Pt was estimated from the Pt(1 1 1) line width using Scherrer's equation with the Gaussian line shape approximation.

2. 3. 3 Transmission electron micrograph (TEM)

TEM images were obtained using a JEOL JEM-2000EX. The accelerating voltage was 200 keV. The samples used for the measurements were pretreated at 400°C in air for 30 min.

2. 3. 4 X-ray photoelectron spectra (XPS)

The XPS measurements were carried out using

a PHI model 5500MC with MgK_α X-rays. The catalyst sample was placed on a grid, and pretreated under 0.1 atm O₂ pressure at 400°C for 15 min. The pretreated sample was cooled to room temperature, and then transferred to the XPS measurement stage.

2. 3. 5 Infrared (IR) spectra

The IR spectra were recorded using a JASCO FT/IR-8900 spectrometer equipped with a diffuse reflectance attachment (JASCO DR-800/H) and an MCT detector. The catalyst sample placed in an *in situ* IR cell with a KBr window was pretreated at 400°C for 20 min in flowing 7 % O₂/N₂ and then cooled to 200°C. The chemisorption of CO was then performed in flowing 0.28 % CO/N₂ at 200°C. The IR spectra of CO adsorbed on the sample were obtained by subtracting the spectra before the CO adsorption from those after the adsorption.

2. 3. 6 CO₂ temperature-programmed desorption(TPD) experiments

The basicity of the zirconia was measured by CO₂-TPD. The TPD experiments were carried out using the same experimental set-up as that used for the activity measurements. An 18 g sample was pretreated at 500°C for 15 min in flowing N₂ (5 l/min), cooled to 100°C, then saturated with a 0.26 % CO₂/N₂ flowing gas mixture. After purging the sample with the N₂ gas, the sample was heated to 400°C at the rate of 50°C/min in flowing N₂ (5 l/min). The concentration of the desorbed CO₂ was analyzed by a nondispersive infrared detector.

3. Results and discussion

3. 1 Catalytic activity

Figs. 1(a) and **(b)** show the conversion of *n*-C₆H₁₄ and SO₂ on the Pt/ZrO₂-8 and Pt/ZrO₂-75 catalysts, respectively, as a function of temperature. The conversion of both on Pt/ZrO₂-8 reached over 80 % at 400°C. In contrast, it is noteworthy that the SO₂ conversion on Pt/ZrO₂-75 is much lower than that on Pt/ZrO₂-8. The Pt/ZrO₂-75 catalyst has only a 20 % SO₂ conversion at 400°C. The temperature at 50 % *n*-C₆H₁₄ conversion on Pt/ZrO₂-75 was 296°C, which was somewhat higher than that (273°C) on Pt/ZrO₂-8. The ΔT shown in Fig. 1 denotes the temperature difference between the 50 % conversion of *n*-C₆H₁₄ and SO₂. The ΔT (203°C) of Pt/ZrO₂-75

was much wider than that (65°C) of Pt/ZrO₂-8. Therefore, the Pt/ZrO₂-75 catalyst has a desirably higher selectivity for the oxidation of *n*-C₆H₁₄ than that of SO₂.

3.2 Arrhenius parameters

The Arrhenius plots for the rates of the *n*-C₆H₁₄ and SO₂ conversions are shown in **Figs. 2**(a) and (b),

respectively. All the data points obtained with the Pt/ZrO₂-8 and Pt/ZrO₂-75 catalysts provide a linear relationship. The apparent activation energy (E_a) and the pre-exponential factor (A) calculated from the Arrhenius plots are summarized in **Table 2**. First, the Pt/ZrO₂-8 and Pt/ZrO₂-75 catalysts have almost same E_a value for the *n*-C₆H₁₄ oxidation,

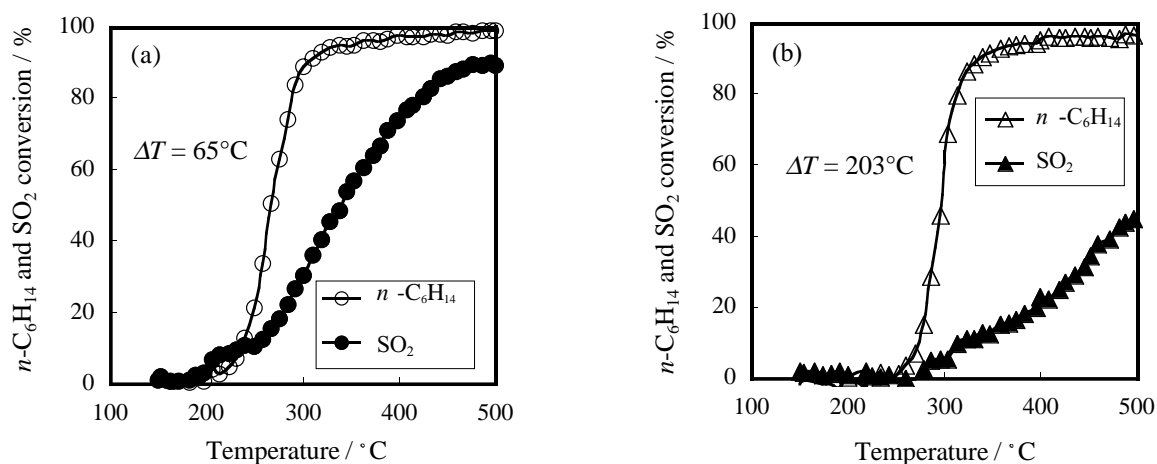


Fig. 1 *n*-C₆H₁₄ and SO₂ conversion efficiency as a function of temperature. (a) Pt/ZrO₂-8, (b) Pt/ZrO₂-75. ΔT denotes the temperature difference between the 50% *n*-C₆H₁₄ and SO₂ conversion efficiencies.

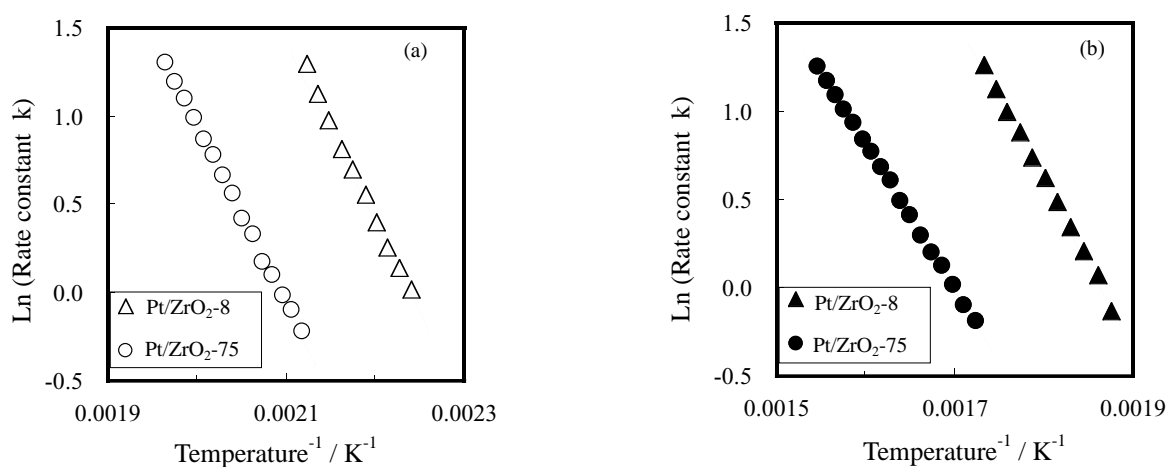


Fig. 2 Arrhenius plots for the oxidations of (a) *n*-C₆H₁₄ and (b) SO₂.

suggesting that these catalysts have identical active sites. On the other hand, the A value for the $n\text{-C}_6\text{H}_{14}$ oxidation on Pt/ZrO₂-8 is one order of magnitude greater than that on Pt/ZrO₂-75. The term A is interpreted as being proportional to the number of catalytic active sites. Thus, an increase in A on Pt/ZrO₂-8 indicates an increase in the number of active sites. Secondly, the E_a for the SO₂ oxidation on Pt/ZrO₂-8 is somewhat higher than that on Pt/ZrO₂-75, but its difference is not much greater, therefore, these catalysts would have identical active sites. As for the A value of the SO₂ oxidation, the same trend as for the $n\text{-C}_6\text{H}_{14}$ oxidation is observed. Based on the results mentioned above, it is suggested that for the oxidation of $n\text{-C}_6\text{H}_{14}$ and SO₂, these catalysts have identical active sites, and that the number of active sites on Pt/ZrO₂-8 is one order of magnitude greater than that on Pt/ZrO₂-75.

Table 2 Apparent activation energies (E_a) and pre-exponential terms (A) for the oxidation of $n\text{-C}_6\text{H}_{14}$ and SO₂ over Pt/ZrO₂ catalysts.

Catalyst	E_a (kcal / mol)		A (1/sec)	
	$n\text{-C}_6\text{H}_{14}$	SO ₂	$n\text{-C}_6\text{H}_{14}$	SO ₂
Pt/ZrO ₂ -8	21	19	3.2×10^{10}	5.6×10^7
Pt/ZrO ₂ -75	20	17	1.4×10^9	1.1×10^6

Table 3 Average platinum particle size of the catalysts estimated by XRD and TEM.

Catalyst	XRD ^a (nm)	TEM (nm)
Pt/ZrO ₂ -8	N.D. ^b	1 - 4
Pt/ZrO ₂ -75	N.D. ^b	N.D. ^c

^a Average particle size was estimated from Pt(1 1 1) line width.

^b The diffraction peak from the Pt particles could not be detected.

^c Pt particles could not be detected in the TEM images.

3.3 Characterization of catalysts

3.3.1 Average platinum particle size of the Pt/ZrO₂ catalysts

Table 3 shows the average platinum particle size of the catalysts estimated by XRD and TEM. The diffraction peaks from the Pt particles in both Pt/ZrO₂-8 and Pt/ZrO₂-75 could not be detected due to their small particle size. The average particle size in Pt/ZrO₂-8 estimated by TEM was 1-4 nm. On the other hand, the Pt particles in Pt/ZrO₂-75 could not be observed even by TEM, suggesting that the Pt particle size in Pt/ZrO₂-75 was less than 1 nm. It is found that the Pt/ZrO₂-75 catalyst has a higher Pt dispersion when compared to Pt/ZrO₂-8.

3.3.2 Oxidation state of Pt in the Pt/ZrO₂ catalysts

Fig. 3 shows the XPS spectra of the catalysts at the Pt 4f band. Metallic Pt (Pt⁰) has Pt 4f_{7/2} and Pt 4f_{5/2} bands at 70.7 and 74.0 eV, respectively¹²⁾. In addition, the binding energy of Pt²⁺ and Pt⁴⁺ is ca. 73.0 and 74.7 eV for 4f_{7/2}, and 76.4 and 78.1 eV for 4f_{5/2}, respectively¹³⁾. The peak assigned to Pt⁰ 4f_{7/2} (70.7 eV) was observed for Pt/ZrO₂-8, while that peak for Pt/ZrO₂-75 almost disappeared. In contrast, the peak assigned to Pt⁴⁺ 4f_{5/2} (78.1 eV) was observed for Pt/ZrO₂-75, but not for Pt/ZrO₂-8. The proportion of Pt⁰, Pt²⁺ and Pt⁴⁺ in the catalysts was quantitatively calculated from the peak fitting of the XPS spectrum (**Fig. 4**). As shown in Fig. 4, the main Pt constituent in Pt/ZrO₂-8 was the Pt⁰ species,

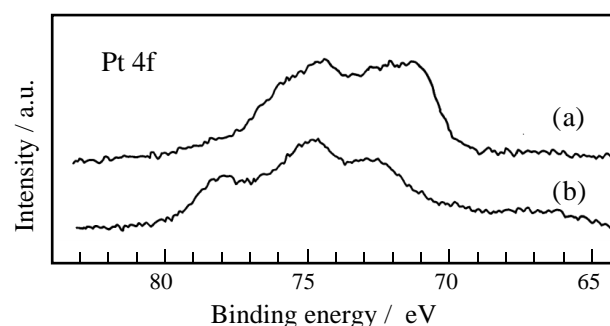


Fig. 3 XPS spectra of the catalysts at the Pt 4f bands. (a) Pt/ZrO₂-8, (b) Pt/ZrO₂-75.

while the Pt^{2+} and Pt^{4+} species with a high oxidation state were mainly present in $\text{Pt}/\text{ZrO}_2\text{-75}$.

Furthermore, we examined the state of Pt by IR using CO as the probe molecule. **Fig. 5** shows the IR spectra of CO adsorbed at 200°C on Pt. The peaks at around $2070\text{-}2090\text{ cm}^{-1}$ observed in both $\text{Pt}/\text{ZrO}_2\text{-8}$ and $\text{Pt}/\text{ZrO}_2\text{-75}$ are assigned to CO adsorbed on Pt^0 ¹⁴⁾. The peak intensity for $\text{Pt}/\text{ZrO}_2\text{-75}$ drastically decreased as compared with $\text{Pt}/\text{ZrO}_2\text{-8}$. This result is in accord with the XPS observation that the proportion of Pt^0 in $\text{Pt}/\text{ZrO}_2\text{-75}$ is much

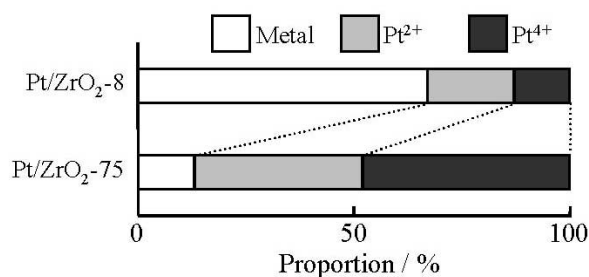


Fig. 4 The proportion of Pt^0 (metal), Pt^{2+} and Pt^{4+} in the catalysts determined by XPS measurements.

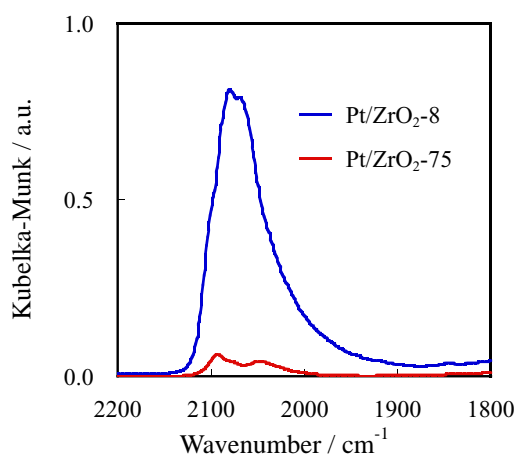


Fig. 5 IR spectra of CO adsorbed at 200°C on the catalysts.

lower than that in $\text{Pt}/\text{ZrO}_2\text{-8}$. We have confirmed that the peak area of the IR is proportional to the amount of CO adsorbed on the catalysts. Therefore, the ratio of the peak area in the IR spectrum is equivalent to that of the number of Pt^0 sites. Consequently, it is found that the number of Pt^0 sites for $\text{Pt}/\text{ZrO}_2\text{-8}$ is about eighteen times greater than that for $\text{Pt}/\text{ZrO}_2\text{-75}$.

3.3.3 Relationship between the basicity of zirconia supports and the oxidation state of Pt

The basicity of the zirconia supports was measured by CO_2 -TPD. The CO_2 -TPD profiles of $\text{ZrO}_2\text{-8}$ and $\text{ZrO}_2\text{-75}$ are shown in **Fig. 6**. The basicity of the $\text{ZrO}_2\text{-75}$ with a high surface area was much higher than that of $\text{ZrO}_2\text{-8}$ having a low surface area, indicating that the basicity is related to the surface area.

Yoshida et al. investigated the support effect on the state of the Pt catalysts by XAFS analysis¹⁵⁾. The Pt on a basic support such as MgO and La_2O_3 is fully oxidized in an oxidative atmosphere, while the Pt on the acidic support contains more metallic Pt. Thus, it could be considered in our system that the high basicity of $\text{ZrO}_2\text{-75}$ stabilized the high oxidation state of Pt such as Pt^{2+} and Pt^{4+} compared to $\text{ZrO}_2\text{-8}$.

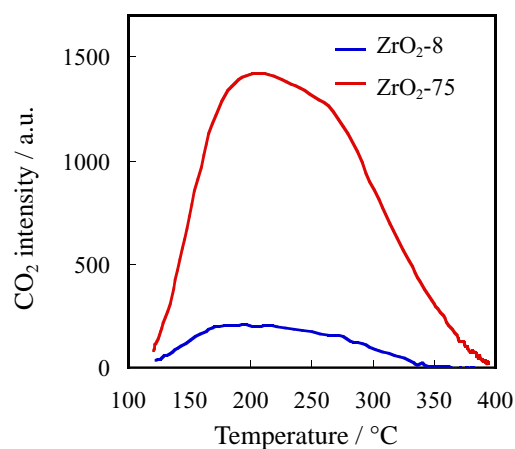


Fig. 6 CO_2 -TPD profiles of the ZrO_2 supports.

3.4 The cause of the reaction selectivity for *n*-hexane and SO₂ oxidations

As mentioned above, the Arrhenius parameter measurements indicated that both catalysts have identical active sites for the complete oxidation of *n*-C₆H₁₄, and that the pre-exponential factor on Pt/ZrO₂-8 is one order of magnitude greater than that on Pt/ZrO₂-75. This same trend applies to the oxidation of SO₂. On the other hand, from the IR peak area of adsorbed CO, the number of Pt⁰ sites on Pt/ZrO₂-8 is at least ten times greater than that for Pt/ZrO₂-75. The correlation between the pre-exponential factor and the Pt⁰ sites indicates that the Pt⁰ sites mainly act as active sites for the *n*-C₆H₁₄ and SO₂ oxidations. Additionally, it is postulated that the difference in the number of Pt⁰ active sites causes the apparent selectivity for the *n*-C₆H₁₄ and SO₂ oxidations to change. Since the reaction rate for the SO₂ oxidation is much slower than that for the *n*-C₆H₁₄ oxidation, the decrease in the active Pt⁰ sites apparently suppresses the SO₂ oxidation compared to the *n*-C₆H₁₄ oxidation. Therefore, the cause of the high selectivity for Pt/ZrO₂-75 is the extreme decrease in the active Pt⁰ site. Furthermore, in order

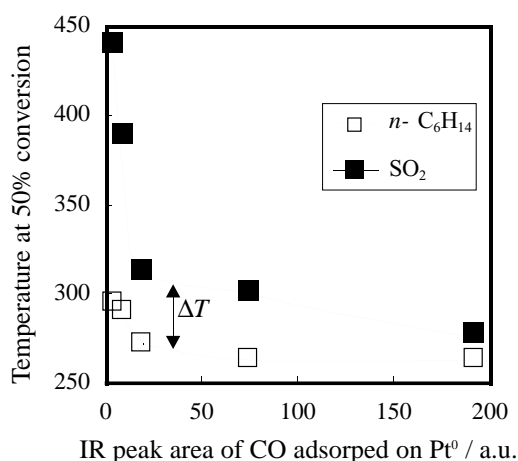


Fig. 7 The relation between the conversion of *n*-C₆H₁₄ and SO₂ oxidation and the amount of the Pt⁰ (metal) site. Pt/SiO₂ catalysts with various amounts of Pt⁰ sites were employed. The IR peak area of CO adsorbed on Pt⁰ is proportional to the amount of the Pt⁰ site. ΔT denotes the temperature difference between the 50 % *n*-C₆H₁₄ and SO₂ conversion efficiencies.

to verify this hypothesis, we estimated the catalytic activity on the Pt/SiO₂ catalysts with various numbers of Pt⁰ sites (**Fig. 7**). These Pt/SiO₂ catalysts were prepared by modifications of the Pt loading amount and calcination temperatures. In addition, it has been reported that most of the Pt on the SiO₂ support exist in the metallic state in an oxidative atmosphere¹⁵. As shown in Fig. 7, the SO₂ oxidation is more suppressed by decreasing the active Pt⁰ sites than the *n*-C₆H₁₄ oxidation, causing ΔT to widen. From these results, it is clear that the apparent oxidation selectivity between *n*-C₆H₁₄ and SO₂ could be controlled by the number of active Pt⁰ sites.

4. Conclusion

In this study, we estimated the reaction selectivity for the *n*-C₆H₁₄ and SO₂ oxidations over two types of Pt/ZrO₂ catalysts with low and high ZrO₂ support surface areas. The Pt/ZrO₂-75 catalyst with a high surface area has a desirably higher selectivity for the complete oxidation of *n*-C₆H₁₄ than that of SO₂, as compared with the Pt/ZrO₂-8 catalyst with a low surface area. Namely, the Pt/ZrO₂-75 remarkably suppresses the SO₂ oxidation as compared with the *n*-C₆H₁₄ oxidation. In order to clarify the cause of this reaction selectivity, we investigated the Arrhenius parameter for these oxidation reactions and characterized the catalysts using XPS, XRD, TEM, IR and CO₂-TPD methods. The number of Pt⁰ (metal) sites in the Pt/ZrO₂-75 was significantly lower than that in the Pt/ZrO₂-8, because the high basicity of the ZrO₂-75 stabilized the high oxidation state of Pt such as Pt²⁺ and Pt⁴⁺. Since the reaction rate for the SO₂ oxidation is much slower than that for the *n*-C₆H₁₄ oxidation, the decrease in the active Pt⁰ site apparently suppresses the SO₂ oxidation as compared with the *n*-C₆H₁₄ oxidation. Therefore, the cause of the high selectivity for the Pt/ZrO₂-75 was the extreme decrease in the active Pt⁰ sites. It was clarified that the apparent oxidation selectivity between *n*-C₆H₁₄ and SO₂ could be controlled by the number of active Pt⁰ sites.

Acknowledgements

This research was completed thanks to Messrs. K. Doumae (XPS), Y. Matsuoka (TEM), Y. Watanabe and K. Banno.

References

- 1) Zelenka, P., et al. : Appl. Catal. B, **10**(1996), 3
- 2) Farrauto, R. J., et al. : Appl. Catal. B, **10**(1996), 29
- 3) Watanabe, Y., et al. : Appl. Clay Sci., **16**(2000), 59
- 4) Nagai, Y., et al. : Jpn. Unexamined Patent Publ., 085600 (1998)
- 5) Nagai, Y., et al. : Appl. Catal. B, in press.
- 6) Siegl, W. O., et al. : Atmospheric Environment, **33** (1999), 797
- 7) Lampert, J. K., et al. : Appl. Catal. B, **14**(1997), 211
- 8) Garetto, T. F., et al. : Catal. Today, **62**(2000), 189
- 9) Kiwi-Minsker, L., et al. : Catal. Today, **59**(2000), 61
- 10) Maillet, T., et al. : Appl. Catal. B, **14**(1997), 85
- 11) Ruth, K., et al. : Appl. Catal. B, **24**(2000), L133
- 12) Kim, K. S., et al. : J. Am. Chem. Soc., **93**(1971), 6296
- 13) Grasset, F., et al. : Mater. Res. Bull., **34**(1999), 2101
- 14) Keiski, R. L., et al. : Stud. Surf. Sci. Catal., **96**(1995), 85
- 15) Yoshida, H., et al. : J. Synchrotron Rad., **6**(1999), 471
(Report received on Dec. 11, 2001)



Yasutaka Nagai 長井康貴

Year of birth : 1967

Division : Research-Domain 31

Research fields : Automotive catalyst

Academic society : Catalysis Society of Japan



Hirofumi Shinjoh 新庄博文

Year of birth : 1955

Division : Research-Domain 31

Research fields : Automotive catalyst

Academic degree : Dr.engng.

Academic society : Catalysis Society of Japan , Chemical Society of Japan, The Society of Chemical Engineers, Japan.

Received the JSME Award in 1995.



Koji Yokota 横田幸治

Year of birth : 1953

Division : Research-Domain 31

Research fields : Automotive catalyst

Academic society : Catalysis Society of Japan , Chemical Society of Japan, The Japan Petroleum Inst., Society of Automotive Engineers of Japan.